Carbon Thin Film Deposition Using High Power Pulsed Magnetron Sputtering

B.M. DeKoven, P.R. Ward, and R.E. Weiss, Intevac, Inc., Santa Clara, CA, and D.J. Christie, R.A. Scholl, W.D. Sproul, and F. Tomasel, Advanced Energy Industries, Inc., Fort Collins, CO; and A. Anders, Lawrence Berkeley National Laboratory, Berkeley, CA

Key Words: High density coating; Plasma; High power pulsed magnetron sputtering; Carbon deposition

ABSTRACT

High power pulsed magnetron sputtering (HPPMS) discharge is a new i-PVD technique. With HPPMS, high plasma densities and highly ionized sputtered materials can be produced. The high power is applied to conventional magnetron cathodes in short pulses (typically 50-150 µs). The magnetron cathode was driven by an experimental pulsed power supply in development by Advanced Energy Industries. The power supply can provide peak power pulses in the megawatt range at a repetition frequency of up to 500 Hz and a pulse width in the range of 50–150 µs. In this paper, the deposition of thin (< 20 nm) films with HPPMS using carbon cathodes in a 6-inch circular magnetron is described. We present evidence for increased plasma ion production compared to continuous D.C. magnetron sputtering. Carbon film densities up to 2.7 g/cm^3 have been measured. The density is significantly increased compared to films grown by PECVD (2.1 g/cm^3) or D.C. sputter deposition (< 2.0 g/cm^3). The current–voltage characteristics of the discharges and thin film characterization are also discussed.

INTRODUCTION

The high power pulsed magnetron sputtering (HPPMS) discharge is an emerging PVD technique [1-12]. The technique allows for production of high density plasma without macroparticle generation. Ionization of the sputtered species has been demonstrated for several target materials [2]. It is anticipated that HPPMS could become an important technique because a number of theoretical and experimental studies [13, 14] have shown that densification of the growing film can be achieved by high ion-to-neutral ratio and high ion energy flux arriving at the substrate surface. The high power in HPPMS is applied to ordinary magnetron cathodes in pulses with short duration of typically some tens of microseconds. These short times are chosen in order to utilize very high power during pulses while suppressing glow-to-arc transition due to time delay of onset of arc mode. Distinction between glow mode and arc mode is possible by time-resolved voltage and current measurements as cathodic arcs have voltages < 50 V [15]. The maximum pulse duty cycle is mainly limited by cooling considerations of the magnetron device.

In this paper we describe the deposition of carbon thin films using HPPMS. The objective is to conduct an evaluation of carbon film deposition using the HPPMS technique for data storage applications. Thin (~ 3 nm) hard carbon films are currently used as protective overcoats on hard disks and read-write heads. The areal density of information stored in disk drive products increased at an amazing rate of over 65% for many years, and continues to accelerate to even greater rates [16]. To accomplish this, the “physical spacing” between the magnetic layers of the disk and read/write sensor of the head must continue to decrease. The magnetic spacing includes the overcoats, lubrication, and the fly height. Thinner overcoats allow the read/write head to be closer to the magnetic layer of the disk. As areal densities greater than 150 Gb/in^2 are achieved, the magnetic spacing will be less than 10 nm and the overcoat thickness must decrease to 1–2 nm.

Carbon overcoats currently used are sputtered or ion-beam deposited diamond-like carbon films doped with hydrogen and / or nitrogen. These films are unable to provide acceptable corrosion protection when the film thickness is less than 2-nm thick. Overcoats need to be tough (hard and elastic), chemically inert, pinhole-free, and compatible with the lubricant. Desired carbon film properties are: density: > 2.7 g/cm^3; thickness range: 1.0-2.5 nm; uniformity over 9.5 cm OD: ± 5%; deposition rate: > 0.5 nm/s; smoothness: < 0.4 nm RMS. The films must also demonstrate required wear and corrosion resistance, and lubricant compatibility. Extensive development efforts will be required for a new film concept.

EXPERIMENT

Figure 1 shows a schematic diagram of the experimental setup. Carbon films were prepared using a planar magnetron having a 160-mm-circular cathode. The chamber was pumped to a base pressure of approximately 2 x 10^{-6} Torr and then argon was flowed to reach an operating pressure ~ 3 mTorr. The aluminum and carbon targets were provided by ORYX Advanced Materials (Fremont, CA). The carbon target was 99.9995% pure graphite with a density of ~1.90 g/cm^3. The carbon target was bonded to a copper backing plate with indium and then bolted to a heat sink. The aluminum targets were also 99.9995% pure and were clamped directly to the heat sink.

© 2003 Society of Vacuum Coaters 505/856-7188

46th Annual Technical Conference Proceedings (2003) ISSN 0737-5921

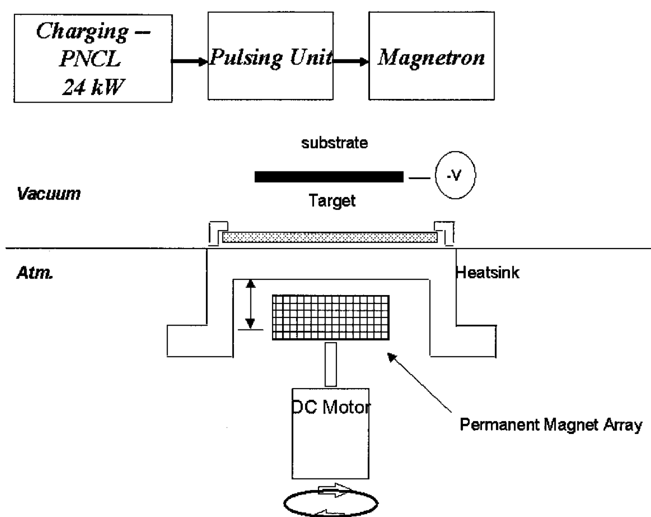

Figure 1: Schematic representation of the experimental setup of the high power pulsing system and magnetron.

The plasma was controlled using an experimental high power pulsed energy source (Advanced Energy Industries). The operating conditions of the power supply for carbon deposition were: pulse width 60-120 μs, pulsing frequency 10-200 Hz, plasma impedance 0.5-3.0Ω, capacitor charging voltage 500-2000 V, and up to 5 kW average power. Typically, the power supply was operated at a duty cycle of 1.4% (100 μs @ 140 Hz). The target voltage was monitored with a high-voltage probe (Tektronix P6061), while target current was measured with a current monitor (Pearson, 1V/kA).

Time resolved emission spectra between 200-800 nm of the magnetron plasma were taken using a 0.3 m spectrometer (Acton Research SpectraPro 300i) using an intensified CCD camera (Princeton Instruments PI MAX512RB). The timing of the high voltage pulse used to gate the optical detection system was synchronized with the high power pulsing system.

The ion/neutral ratio for the deposited material was measured using a quartz crystal microbalance (QCM) mounted behind a two layer-gridded energy analyzer with an aperture limiting mask [17]. This measuring device was located in the horizontal plane of the substrate. Grid 1, grid 2, and mask are located 0.9 cm, 1.3 cm, and 2.4 cm from the crystal surface. The gridded analyzer was located 7.5 cm from the magnetron target. The analyzer mask was grounded, the top grid was set to -100 V and the bottom grid was biased at either ±40 V. Each grid consists of a mesh with holes of 0.094 ± 0.004 mm diameter; the geometric transmittance of the grid was 52.7 ± 2.1%. When grid 1 was biased to -40 V, both positive ions and neutrals deposited onto the crystal. The deposition rate of ions and neutrals can be determined using a deposition controller (MDC 260; Maxtek, Inc.). When grid 1 was biased +40 V, positive ions are repelled and only neutral species deposit. The ionization fraction is calculated using the ratio of the two measurements.

Carbon film stress was measured using a wafer measurement system (model FSM128; Frontier Semiconductor Measurement Inc.). First, the curvature of an uncoated wafer was measured. Following deposition, the FSM128 was used to measure the change of curvature induced in a wafer due to the deposited film. The deposited film thickness and reference curvature data for the uncoated Si wafer were used to calculate the film stress. The FSM128 can measure stress as low as several MPa. The carbon film thickness was obtained using a profilometer (Model P-10 Surface Profiler; KLA Tencor).

X-ray reflectivity, AFM, XPS, and nano-indentation measurements were also performed on a variety of carbon films. The data was obtained from several different analytical service companies as mentioned in the acknowledgements section. Further details of these methods will be reported elsewhere [18].

RESULTS AND DISCUSSION

HPPMS Carbon Plasma Characteristics

The HPPMS discharge for carbon using the 6-inch cathode was operated with a duty cycle of 1.4% at a frequency of 140 Hz. HPPMS of carbon in an Ar atmosphere with peak power 300 kW was conducted using an average power up to 5 kW maximum. HPPMS discharge voltages of 700 V and currents up to 300 A were achieved with minimal arcing (< 10% of pulses).

Figure 2 shows the carbon plasma characteristics during HPPMS as a function of time for several power supply capacitor charging voltages. Pulses, 175 μs of total duration, have a FWHM of 100 μs. Figures 2 a-d show the oscilloscope traces for the plasma voltage, current, power, and impedance, respectively. The voltage (Figure 2a) was always initially high and oscillated during the first 50 μs, which helps to ignite the plasma. The plasma current oscillated in synchronization with the voltage, but at lower values compared to the peak current achieved during the pulse. During the ignition period the plasma impedance (Figure 2d) varied dramatically (up to 50 Ω) and was quite high compared to stable values of 3-5 Ω from 50-150 μs. As the plasma decays to zero power at the end of the pulse, the impedance monotonically increases since the plasma current is dropping much more rapidly than the voltage.

a.

b.

c.

d.

Figure 2: HPPMS carbon plasma characteristics.

The oscillations in the plasma properties shown in Figure 2 qualitatively depend upon the magnetic field and shielding used in the magnetron. Using different cathodes implies big differences in cooling, peak power, and required shielding. Strong and weak magnetic fields greatly influence HPPMS cathode operation. Shield volume is critical due to changing cathode sheath at different power densities.

More insight regarding the nature of the high power pulsed plasma can be obtained by examining the discharge current-voltage characteristics. Figure 3 shows the discharge voltage vs. current density for several different magnetrons using either aluminum or carbon targets. The I-U data for each case is fit to the power law $I = kU^n$ [19, 20] which is characteristic for DC magnetrons. The comparison between carbon and aluminum is useful since there are differences in both the sputter yield and ionization cross section between aluminum and carbon. Data for Al is shown for different size cathodes, and DC vs. HPPMS. For the Al plasma operating in a DC mode, n = 8.3, which is quite characteristic of DC plasma. For the Al plasma in a pulsed mode, the slope of the power law fit showed different n values depending upon the size of the cathode. For Al using the 2.5-inch cathode under pulsed operation, n = 2.2. However, for Al using the 6-inch cathode, n remained at 8.1 even for pulsed operation. The plasma I-U characteristics for carbon using a 6-inch cathode under pulsed operation showed n-values identical to Al.

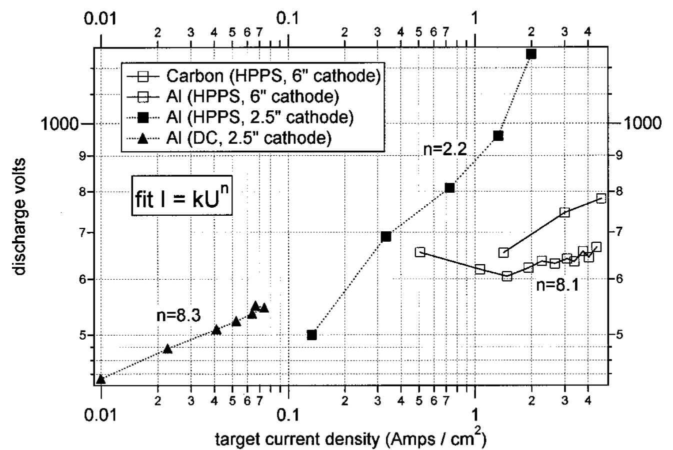

Figure 3: Discharge voltage vs. current comparison.

Ehiasarian et al. [2] reported that the exponent changes to 1 during high power pulsed sputtering using Cr cathodes, and a similar result was reported when using a small W target [21]. A possible interpretation of lowering the n value is that a transition to a fully ionized plasma occurs. The sputtered atoms become increasingly ionized, enhancing their contribution to the plasma density. The observations for 6-inch circular magnetron configurations for both C and Al shown in Figure 3 indicate conventional magnetron behavior even when the plasma is pulsed. A proposed model for predicting the self-sputter-rate [21] indicates low sputter yields for C and Al at the plasma voltages observed. It is not fully understood at this time why there are differences between magnetron cathode sizes. Obviously, one has to consider current and power densities, rather than absolute values, but different magnetic field strengths may also play a key role. A higher magnetic field strength can produce and maintain a higher plasma density, with consequences for the longitudinal and perpendicular conductivity, hence power dissipation. Due to the three-dimensional nature of the field structure, these effects are difficult to model and may sensitively depend on the balancing of the magnetic field.

Figure 4 shows optical emission spectra from DC and pulsed magnetron discharges using 6-inch carbon targets. For regulated DC power operation at 1 kW, strong emission from Ar I (neutral) and Ar II (singly charged ion) completely dominate the spectrum. For DC operation, carbon line emission cannot be distinguished from the background noise. The lower spectrum in Figure 4 is obtained through pulsed operation and is time integrated during the pulse. For approximately the same average power, the spectrum shows that the ionization degree of the plasma formed by pulsing the carbon target is higher. Note that C II (singly charged carbon ions) lines can be identified, but at very low intensity. Qualitatively, there are more ions (both Ar^+ and C^+) for pulsed operation compared to DC operation. The low sputtering yield of carbon and relatively high excitation and ionization energies are likely to be the main causes for the absence or low intensity of carbon emission lines.

Using the 6-inch circular magnetron, the measurements with the gridded quartz crystal monitor (QCM) indicate an ion to neutral ratio of 4.5% ± 0.5% for carbon and 9.5% ± 0.5% for aluminum. The values are much lower than what has been reported for other HPPMS experiments. However, these low ratios are consistent with the HPPMS plasma discharge characteristics, which appeared to be similar to conventional magnetrons, as shown in Figure 3 and previously discussed. One interpretation is that when using a 6-inch target for these materials, the current and power density is not yet high enough to enter the region of fully ionized plasma. Furthermore, carbon and aluminum are light elements, which typically have low self-sputtering yields. Therefore the concentration of sputtered atoms in the plasma is low. Yet another argument is that light elements such as carbon have a relatively high ionization potential and, thus, they cannot be as easily ionized as for example Cr or W as reported in the literature [2, 21]. One can anticipate that optimized magnetic fields, target material and shape, and shielding will influence the control of the HPPMS carbon discharge, though it is open at this time whether a HPPMS regime of ionized carbon can be obtained.

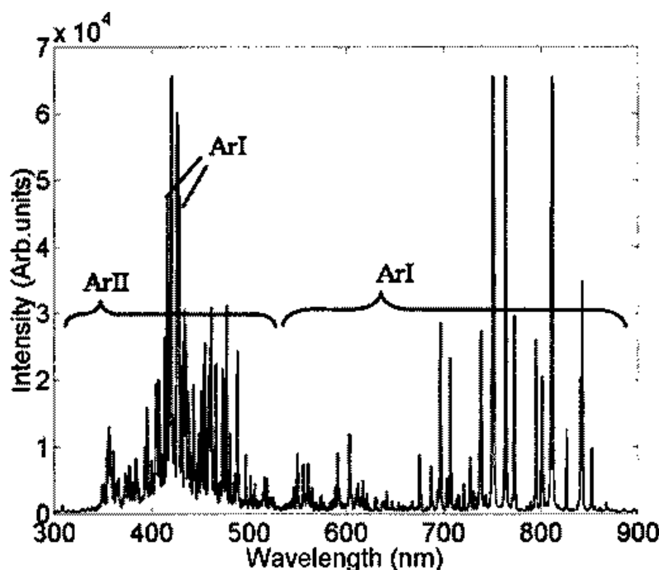

a.

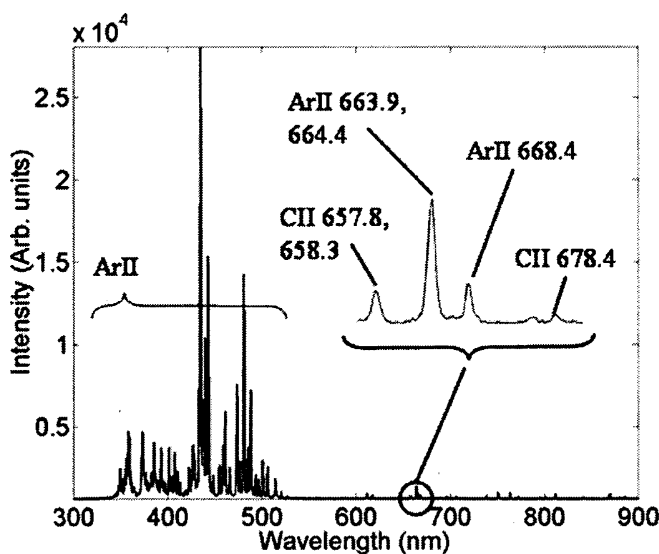

b.

Figure 4: Carbon plasma emission spectra for (a) DC operation and (b) HPPMS operation.

HPPMS Carbon Film Characterization

Table 1 shows the carbon film density and roughness determined by x-ray reflectivity measurements. These film properties are determined from the critical angle and fringe intensity. Both NiP / Al and Si wafer substrates were used. The model

Table 1: Carbon film properties.

Sample ID	Layer Description	Thickness (nm)	Roughness (nm)	Density (g/cm^3)
DC Carbon on NiP/Al disk	Ni Substrate	—	0.8 ± 0.02	7.83 ± 0.02
	carbon Film	32.2 ± 0.4	1.4 ± 0.03	2.04 ± 0.08
HPPMS carbon on NiP/Al disk	Ni Substrate	—	4.8±0.2	7.83 ± 0.02
	Carbon film	25.1 ± 0.1	0.57 ± 0.08	2.67 ± 0.06
	Carbon contamination	2.3 ± 0.2	0.79 ± 0.13	1.43 ± 0.10
HPPMS carbon on Si wafer	Si Substrate	—	0.0 ± 0.5	2.33 ± 0.07
	SiO_2 Film	1.5 ± 1.3	0.001 ± 0.1	2.27 ± 0.05
	Carbon film	26.0 ± 0.1	0.27 ± 0.03	2.73 ± 0.05

for the reflectivity includes fixing the density of the substrate to match the large intensity observed above the critical angle. For HPPMS carbon the film density is significantly higher than the DC deposition case (2.7 g/cm^3 vs. 2.0 g/cm^3). In addition, the roughness of the HPPMS carbon is lower than that for the carbon film deposited using DC regulated power. For the HPPMS carbon, a carbon contamination layer due to atmosphere exposure is added to the model. This is not necessary for DC carbon and may be due to the lower film density and its closeness to the adventitious layer.

Film stress (compressive) was measured for films having the properties in Table 1. The properties are briefly summarized here. The stress is 0.2 GPa for DC-sputtered carbon films compared to 6.0 - 7.0 GPa for HPPMS-carbon. The average composition of the HPPMS carbon is: C - 84.8% ; O - 10.0%; Ar - 3.0%; and H - 2.2%, using XPS for measuring C, O, and Ar, and hydrogen forward scattering for hydrogen. The O content of the film could be due to water absorption and reaction due to exposure to the atmosphere. The average RMS roughness for HPPMS carbon on Si wafer substrates using AFM is 0.30 nm, which agrees well with the XRR roughness.

Table 2 shows the results of characterization for HPPMS and DC carbon based on stress and Raman spectroscopy as a function of increasing sample bias. Both the stress and I_d/I_g peak ratio increase for increasing bias. Also indicated in Table 2 is the sp^3 content based on I_d/I_g estimated following Robertson [22, 23]. For HPPMS carbon films, an increase in the substrate bias leads to higher stress and lower sp^3 content carbon. The observation of high stress and low sp^3 content is quite surprising. Acceleration of ionized carbon to the substrate can produce hard, dense, and highly stressed overcoats resulting from high concentrations of tetrahedral and high sp^3 content. Note that for carbon films, high ion energy (> 200 eV) has been reported to reduce both stress and sp^3 content [24, 25].

Figure 5 shows AFM images (10-µm x 10-µm scan area, 50-nm height) for HPPMS carbon films. Figure 5a shows the

Table 2: Stress and Raman characterization of carbon films.

Condition	Stress (GPa)	I_d/I_g	sp^3 fraction
HPPMS Bias = -175 V Current = 0.8 mA	6.5	1.947	0.20 – 0.25
HPPMS Bias = -175 V Current = 0.8 mA	5.7	1.458	0.30 – 0.35
HPPMS Bias = -125 V Current = 0.8 mA	4.7	1.200	0.35 – 0.40
HPPMS Bias = -125 V Current = 0.2 mA	3.6	0.708	0.40 – 0.45
DC Bias = -100 V	1.6	1.080	0.35 – 0.40

image of a thin film (5-nm thick) and Figure 5b is the image of a thick film (150-nm film). There is a striking difference in the film morphology for the two different thicknesses. The thick film contains a high density of features (0.1-0.2 μm) which protrude from the surface. These features are also present on the thin film, but are much less abundant. Although not shown, these features increase in density for films between 5- and 150-nm thickness.

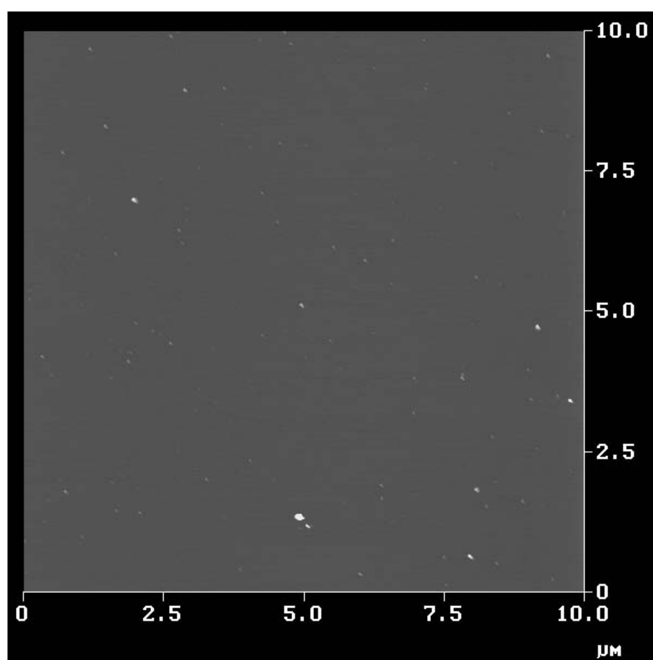

a.

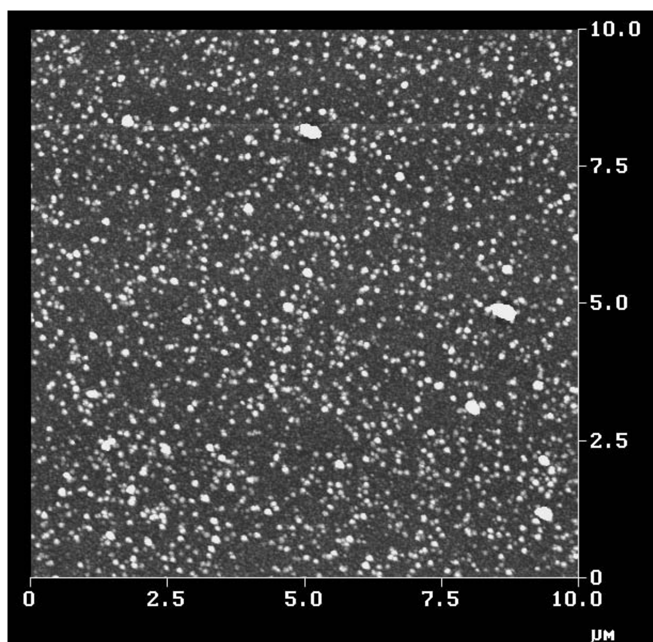

b.

Figure 5: AFM top-view images for 5-nm and 150-nm thick films.

The mechanism leading to the features present in Figure 5 is unclear at the present time. It is tempting to believe that the abundant features on the HPPMS carbon surfaces are due to macroparticles produced by the short (though terminated or suppressed) arcs. Figure 6 shows the AFM image (10-μm x 10-μm scan area, 50-nm height) of a "crack" on a 35- nm-thick film. Again, the protruding surface features are observed. However, the features appear to decorate a crack. There is no obvious reason why macroparticles should decorate a crack, or what even appears to be a crack. It is conceivable that we see two different things that have similar appearance: 1) macroparticles, produced at cathode spots and 2) growth defects, produced on the surface by stress relief. An argument for 1) is the size distribution: it is known that smaller particles are more frequent than larger ones, with an approximate exponential law. An argument for 2) is that such alignment of "particles" cannot occur by randomly arriving particles. There are other interpretations for the defects other than macroparticles. Although not shown, we have observed features which look like "holes" in the center of some these surface features. Another possible hypothesis is that nano-argon bubbles form close under the surface, causing the creation of "roughness" that looks particle-like when the bubbles burst and argon is released back to above the substrate surface. There may be several "real" explanations, including that the structure is not amorphous but nano-crystalline, and the shapes follow nano-grain boundaries.

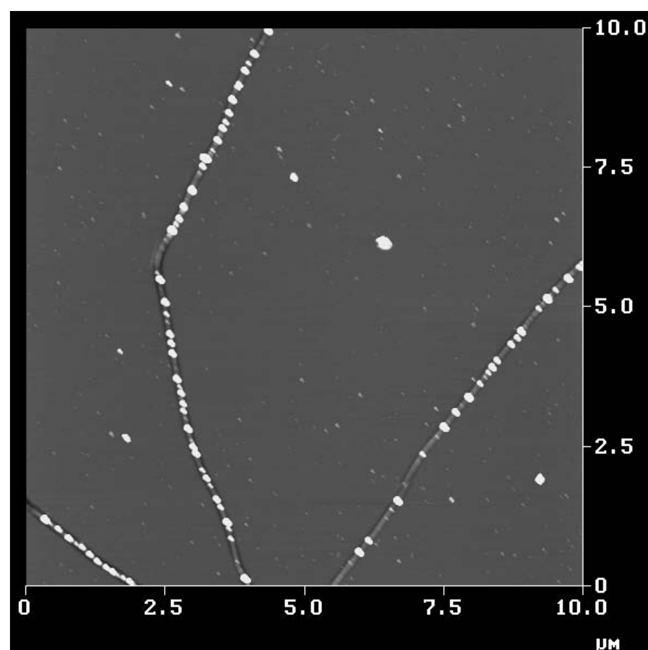

Figure 6: AFM image of decorated crack on HPPMS carbon film (35 nm thick).

Nano-indentation was also conducted on several films that were 150-nm thick. The results for HPPMS carbon (bias = 175 V, stress ~ 5.5 GPa) show hardness and modulus of 6.9 GPa and 61.1 GPa, respectively. The measured hardness should be considered low based on film stress for carbon films [23, 24]. Film thickness was 150 nm to insure that substrate effects do not influence these values. However, the low hardness and stress is most likely due to the surface morphology described previously.

CONCLUSIONS

High carbon film density (2.7 g/cm^3) was achieved which is most likely due to high Ar ion content of high powered pulsed plasma and atomic peening during the deposition. The HPPMS carbon film is graphite-like with sp^3 fraction estimated to be 0.20 – 0.30. The hardness was found to be only about ~ 7 GPa, compared to 25 GPa for PECVD films. This surprisingly low hardness value may be due to the unique film morphology of thick films, and may not apply to the thin films, which are of interest to data storage applications.

It was shown that high-density carbon can be produced by HPPMS. Emission spectroscopy indicates a greatly enhanced degree of ionization of the sputtering plasma, although the ionization of carbon appears to be low. Therefore, it is likely that atomic peening by argon ions is largely responsible for carbon film densification. To some degree, carbon ions in the plasma may also contribute to the increase in film density. Although the HPPMS carbon films are characterized by high density and high stress, in terms of bonds they may be better described as graphite-like rather than diamond-like. This combination of properties might offer good corrosion resistance and good lubricity for data storage applications. There is still a great need for better understanding of the mechanism of film formation. We believe that HPPMS is a new frontier in thin film coating technology. HPPMS may offer a new technique to produce and control film growth, leading to structure and properties of coatings that can be used, for example, in the data storage industry.

ACKNOWLEDGEMENTS

We acknowledge B. Kakimoto and C. Marion of Intevac for assistance with carbon film deposition. D. Carter and K. Peterson of Advanced Energy Industries are acknowledged for assistance with the experimental high power pulsed energy source. We acknowledge contributions towards carbon film characterization from the following individuals: C. England, B. Burrows, and S. Shourie of Materials Analytical Services (Sunnyvale, CA) for XRR, AFM, XPS, and HFS characterization; A. Strom of Hysitron (Minneapolis, MN) for nano-indentation; and H. Gotts of the Analytical Services Group (Santa Clara, CA) for Raman spectroscopy.

REFERENCES

1. V. Kouznetsov, K. Macak, J.M. Schneider, U. Helmersson, I. Petrov, Surf. Coating Technol. 122 (2.3) (1999) 290.
2. A.P. Ehiasarian, R. New, W.-D. Munz, L. Hultman, U. Helmersson, V. Kouznetsov, Vacuum 65 (2002) 147.
3. A.P. Ehiasarian, K.A. Macak, C. Schonjahn, R. New, W.-D. Munz, 44th Annual Technical Conference Proceedings of the Society of Vacuum Coaters, p. 382, 2001.
4. W.-D. Munz, D.B. Lewis, P.E. Hovsepian, C. Schonjahn, A. Ehiasarian, I.J. Smith, Surf. Eng. 17 (1) (2001) 15.
5. V. Kouznetsov, U.S. Pat. # 6,296,742B1, October 2, 2001.
6. A. P. Ehiasarian, W. -D. Münz, L. Hultman, U. Helmersson and I. Petrov, Surf. Coating Technol. 163-164, (2003) 267.
7. Karol Macák, Vladimir Kouznetsov, Jochen Schneider, Ulf Helmersson, and Ivan Petrov., J. Vac. Sci. Technol. A 18 (2000) 1533.
8. S. M. Rossnagel and J. Hopwood, J. Vac. Technol. B 12 (1994) 449.
9. J. Hopwood, Physics of Plasmas 5 (1998) 1624.
10. I. Petrov, L. Hultman, U. Helmersson, J.E. Sundgren, J.E. Greene, Thin Solid Films 169 (2) (1989) 299.
11. L. Hultman, W.-D. Munz, J. Musil, S. Kadlec, I. Petrov, J.E. Greene, J. Vac. Sci. Technol. A 9 (3) (1991) 434.
12. C. Schonjahn, L.A. Donohue, D.B. Lewis, W.-D. Munz, R.D. Twesten, I. Petrov, J. Vac. Sci. Technol. A 18 (4) (2000) 1718.
13. K.-H. Müller, J. Appl. Phys. 59 (1986) 2803.
14. W. Möller, Thin Solid Films 228 (1993) 319.
15. A. Anders, B. Yotsombat, and R. Binder, J. Appl. Phys. 89 (2001) 7764.
16. P. R. Goglia, J. Berkowitz, J. Hoehn, A. Xidis, and L. Stover, Diamond Rel. Mater. 10 (2001) 271.
17. M. C. Allain, D. B. Hayden, D. R. Juliano, and D. N. Ruzic, J. Vac. Sci. Technol. A 18 (2000) 797.

18. B.M. DeKoven, P.R. Ward, R.E. Weiss, D.J. Christie, R.A. Scholl, W.D. Sproul, F. Tomasel, A. Anders, to be published.

19. J. R. Roth, Industrial Plasma Engineering. Vol. 1: Principles (Bristol and Philadelphia: Institute of Physics Publishing, 1995).

20. W.D. Westwood, Sputter Deposition, AVS Education Committee Book Series, Vol. 2, American Vacuum Society (2003) 57.

21. A. Anders, presented at The International Conference on Metallurgical Coatings and Thin Films, San Diego, May 2003.

22. A.C. Ferrari and J. Robertson, Phys. Rev. B 61 (2000) 95.

23. J. Robertson, Diamond Rel. Mater. 2 (1993) 984.

24. S. Anders, D. L. Callahan, G. M. Pharr, T. Y. Tsui, and C. S. Bhatia, Surf. Coat. Technol. 94/95 (1997) 189.

25. M. M. M. Bilek, R. N. Tarrant, D. R. McKenzie, S. H. N. Lim, and D. G. McCulloch, "Control of stress and microstructure in cathodic arc deposited films," Proceedings of XXth Int. Symp. on Discharges and Electrical Insulation in Vacuum, Tours, France, (2002) 95.